The Canadian Mineralogist
Vol. 40, pp. 1705-1716 (2002)

PHASE-EQUILIBRIUM CONSTRAINTS ON THE MAGMATIC ORIGIN OF LAURITE + Ru–Os–Ir ALLOY

DAVID R.A. ANDREWS AND JAMES M. BRENAN§

Department of Geology, University of Toronto, Toronto, Ontario M5S 3B1, Canada

ABSTRACT

To more completely assess the origin of associated laurite (RuS_2) and Ru–Os–Ir (IPGE) alloy which are found as inclusions in near-liquidus phenocrysts such as chromian spinel, we conducted experiments to evaluate the effects of T and $f(S_2)$ on phase relations in the system Ru–Os–Ir–Cu–S. Cu–S melt (added as a flux) + IPGE metals were held in silica crucibles, and experiments were done in both vertical-tube gas-mixing furnace apparatus [low $f(S_2)$] and evacuated silica tubes [higher $f(S_2)$ buffered by Pt–PtS] at 1200–1250°C for 1–3 days. At constant $f(S_2)$ of 10^{-1} atm, the two-phase field of laurite + alloy is restricted to only the most Ru-rich bulk compositions ($X_{Ru} > 0.85$) at 1250°C, and slightly expands to encompass more Ru-poor compositions ($X_{Ru} > 0.6$) at 1200°C. At this $f(S_2)$, laurite remains very close to pure RuS_2. An increase in sulfur fugacity to $10^{-0.39}$ atm at 1200°C and $10^{-0.07}$ atm at 1250°C resulted in a considerable expansion of the two-phase field, with both laurite and alloy dissolving more Os + Ir. For example, at 1250°C and $f(S_2)$ of $10^{-0.07}$, the Os and Ir content of laurite increases to ~20 and ~12 at.%, respectively. Coexisting alloys in both sets of high-$f(S_2)$ experiments contain less than 15 at.% Ru. The compositions of laurite and IPGE alloy defined by high-$f(S_2)$ experiments show remarkable similarity to coexisting PGM compositions preserved in natural chromitite from several localities. If such phases are the product of entrapment at the magmatic stage, then high-$f(S_2)$ conditions are inferred. Similarly, the bulk compositions of laurite from suites in which IPGE alloy is absent also suggest similarly high $f(S_2)$, if high-temperature entrapment is assumed. Limits on the $f(O_2)$ of magmas that may precipitate alloy–laurite pairs stem from the requirement that such magmas remain sulfide-liquid-undersaturated, at least until PGM are trapped in their phenocryst host. Calculations suggest that for this to occur at high $f(S_2)$, laurite + IPGE alloy precipitation requires the involvement of relatively oxidized, low-FeO magmas.

Keywords: laurite, alloy, platinum-group elements, phase equilibria.

SOMMAIRE

Afin d'évaluer plus complètement l'origine de la laurite (RuS_2) et de l'alliage Ru–Os–Ir (éléments du groupe du platine du sous-groupe de l'iridium, IPGE) associés en inclusions dans les phénocristaux formées près du liquidus, tel le spinelle chromifère, nous avons évalué expérimentalement les effets de la température et de la fugacité de soufre sur les relations de phase dans le système Ru–Os–Ir–Cu–S. Le bain fondu Cu–S (ajouté sous forme de fondant) + les métaux IPGE ont été chauffés dans un récipient en silice, et les expériences ont été faites soit dans un four vertical conçu pour mélange de gas [faible $f(S_2)$], soit dans des tubes de silice évacués [$f(S_2)$ plus élevée, tamponnée par le couple Pt–PtS] à 1200–1250°C pour 1–3 jours. A $f(S_2)$ constante de 10^{-1} atmosphère, le champ à deux phases laurite + alliage est restreint aux seules compositions globales les plus riches en Ru ($X_{Ru} > 0.85$) à 1250°C; il augmente pour inclure des compositions à plus faible teneur en Ru ($X_{Ru} > 0.6$) à 1200°C. A cette valeur de $f(S_2)$, la laurite demeure très proche du pôle RuS_2. Une augmentation de la fugacité de soufre jusqu'à $10^{-0.39}$ atmosphère à 1200°C et $10^{-0.07}$ atmosphère à 1250°C mène à une augmentation considérable du champ à deux phases, la laurite et l'alliage acceptant des quantités accrues de Os + Ir. A titre d'exemple, à 1250°C et $f(S_2)$ égale à $10^{-0.07}$, la teneur en Os et Ir de la laurite augmente à ~20 et ~12 at.%, respectivement. Les alliages coexistants dans les deux séries d'expériences à $f(S_2)$ élevée contiennent moins de 15 at.% Ru. Les compositions de laurite et d'alliage IPGE dans ces expériences à $f(S_2)$ élevée montrent des ressemblances remarquables avec celles des minéraux du groupe du platine coexistants dans la chromitite à plusieurs endroits. Si de telles phases sont piégées à un stade magmatique, une valeur élevée de $f(S_2)$ semble indiquée. De même, les compositions globales de la laurite provenant des suites dépourvues d'un alliage IPGE indiquent elles aussi des valeurs élevées de $f(S_2)$, si le piégeage s'est fait à température élevée. Les limites que nous pouvons placer sur la $f(O_2)$ des magmas aptes à précipiter des paires alliage–laurite découlent de l'exigeance que ces magmas doivent rester sous-saturés en liquide sulfuré, du moins jusqu'au stade où les minéraux du groupe du platine sont piégés dans leur hôte phénocristique. D'après nos calculs, et acceptant que ce phénomène se déroulerait à $f(S_2)$ élevée, la précipitation de laurite + alliage IPGE requiert l'implication d'un magma relativement oxydé, et à faible teneur en FeO.

(Traduit par la Rédaction)

Mots-clés: laurite, alliage, éléments du groupe du platine, équilibres des phases.

§ *E-mail address*: brenan@geology.utoronto.ca

Introduction

The most common platinum-group minerals (PGM) in mafic and ultramafic igneous rocks are laurite (RuS_2) and Ru–Os–Ir alloy (*e.g.,* Legendre & Augé 1986). The occurrence of these minerals as inclusions within primary liquidus phases (olivine and chromian spinel), combined with their high thermal stability (Brenan & Andrews 2001a, b), and their low solubility in mafic silicate melts (Borisov & Palme 1995, 2000, Borisov & Nachtweyh 1998, Borisov & Walker 2000), lend plausibility to the notion that they may be early-formed phenocrysts. However, other observations have cast doubt on the high-temperature origin of these minerals. In particular, they occur with base-metal sulfides; if interpreted as crystallized sulfide liquid, such a liquid should have completely dissolved these PGM at supersolidus conditions (Andrews & Brenan 2002, Ballhaus & Ulmer 1995). In addition, laurite and an alloy of iridium-subgroup platinum-group elements (IPGE) occur with other PGM (*i.e.,* various arsenides and tellurides) that are considered to have a low-temperature origin, or belong to a hydrothermal paragenesis. Inasmuch as the early crystallization of Ru–Os–Ir-rich PGM would account for the observed fractionation of the IPGE from Rh, Pt, and Pd (the PPGE) in mafic igneous rocks, establishing the timing of their formation is of importance to understanding the geochemistry of the PGE in such rocks.

Using a simple thermodynamic analysis, Brenan & Andrews (2001a) showed that for a particular bulk-composition, laurite will be more Ru-rich than the coexisting alloy, and the compositions of both laurite and alloy will become (Os + Ir)-rich and Ru-poor with increased $f(S_2)$ or decreased T. Our initial experimental results are consistent with predictions, although we could not reproduce the compositions of coexisting laurite and alloy from natural parageneses. Specifically, we found that both natural laurite and coexisting alloy have far more Os + Ir than that produced in our experiments at 1200–1250°C and log $f(S_2)$ of –0.9 to –1.3. If laurite + alloy are trapped in growing phenocrysts at magmatic temperatures, then $f(S_2)$ must be higher than in our experiments. In this paper, we present results of phase-equilibrium experiments designed to provide a more complete assessment of the stability of laurite + IPGE alloy. We have investigated a larger range in both $f(S_2)$ and bulk composition than we did earlier (Brenan & Andrews 2001a), and here show that the composition of natural laurite–alloy pairs is consistent with formation at magmatic temperatures, provided $f(S_2)$ is high ($10^{-0.39}$ to $10^{-0.07}$ atm).

Experimental Overview

Our overall goal in this study was to conduct a series of experiments to determine the effect of temperature and sulfur fugacity on the phase relationships in the ruthenium–osmium–iridium ternary system. These data are used to construct phase diagrams to illustrate the extent of the two-phase field of coexisting laurite + alloy, and to determine how coexisting compositions shift with T and $f(S_2)$. We employed two different experimental techniques to control sulfur fugacity: gas mixing and solid buffers. The highest fugacity of sulfur that can be imposed in our gas-mixing apparatus is approximately $10^{-0.85}$ atm at temperatures between 1200 and 1250°C. Consequently, experiments in which a higher fugacity of sulfur was desired were run in evacuated silica tubes and employed the Pt–PtS buffer. The two-phase field of laurite and Ru–Os–Ir alloy has been determined by employing bulk compositions on both the Ru–Os and Ru–Ir binary systems, in addition to those that lie in the Ru–Os–Ir ternary system. In all experiments, we employed molten Cu sulfide as a flux for synthesizing phases, and fused silica as a container. In reconnaissance studies, we have observed that the IPGE are only slightly soluble in copper sulfide liquid (<0.5 wt%), thus bulk-solid compositions remained close to the IPGE metal mixture added initially. Furthermore, we found that Cu does not partition readily into IPGE phases (≤1.5 wt% in alloy and laurite). Thus any effect of Cu on the phase relations is likely to be minimal. An additional benefit of using molten Cu sulfide is that it showed no signs of reaction with the silica container, unlike FeS, which rapidly reacts to form a melt of fayalite composition at similar temperatures.

Gas-Mixing Experiments

In the gas-mixing experiments, we employed a modified 1-atm vertical tube furnace using mixtures of CO, CO_2, and SO_2 gases to control the fugacities of oxygen and sulfur; the furnace design is similar to that described in Brenan & Caciagli (2000). Initial bulk-compositions were made by mixing desired proportions of IPGE metal powders (15 mg total) with 40–50 mg of Cu metal powder. Each mixture was then loaded into a silica crucible, which was part of an array of 3–4 crucibles. This sample array enabled us to run several bulk compositions in the furnace simultaneously, thus allowing compositional effects to be determined at identical conditions of T, $f(O_2)$ and $f(S_2)$. In each experiment, starting compositions contained similar total Ru contents, and each of the Ru–Os, Ru–Ir and Ru–Os–Ir systems were investigated at the same time.

Sample holders were suspended from a hook fashioned at the end of a silica rod measuring 60 cm in length and 3 mm in width. In a typical experiment, the silica rod was retracted so that the sample holder was initially positioned in the upper cool region of the furnace. The furnace was then sealed, and gas flow commenced. After 20 to 30 minutes, the rod was lowered to position the holder within the predetermined hot-spot of the furnace assembly, where samples remained for 70–79 hours. A revised version of the program COHSmix, kindly supplied by Victor Kress, was used to calculate the values

of $f(O_2)$ and $f(S_2)$ in this paper. The accuracy of the sulfur fugacity quoted was assessed 1) by using the pyrrhotite sulfur barometer of Toulmin & Barton (1964) at 900°C and log $f(S_2)$ of –1.5, –2 and –3, and 2) by determining the $f(S_2)$ of the Ru–RuS_2 equilibrium at 1200°C. Oxygen fugacity was checked using the stability of solid oxide buffers (nickel–nickel oxide, molybdenum – molybdenum oxide, iron–wüstite), and we have also employed the NiO–Pd redox sensor at 1000°C (Pownceby & O'Neill 1994). On the basis of this assessment, we estimate $f(S_2)$ and $f(O_2)$ accuracy to be within 0.3 log units. A summary of experimental results, listing starting compositions, is given in Table 1.

Evacuated-Silica-Tube Experiments

Evacuated-silica-tube experiments used a Pt–PtS assemblage to buffer sulfur fugacity, as defined by the reaction:

$$Pt + \tfrac{1}{2}\, S_2 = PtS \qquad (1)$$

Values of sulfur fugacity buffered by this assemblage were calculated at a given temperature using the thermodynamic data of Barin (1995). Evacuated-silica-tube experiments were conducted at 1200 and 1250°C; the log $f(S_2)$ buffered by reaction (1) at these temperatures is calculated to be –0.39 and –0.07, respectively. Platinum sulfide was synthesized in evacuated silica tubes using stoichiometric mixtures of Pt and S. The synthesis of PtS involved loading the Pt + S mixture, sealing the tube under vacuum, then heating the sample to 650°C for 24 hours, followed by a temperature increase to 1100°C over 6 hours and isothermal "soaking" for an additional 24 hours. The sample was quenched in a cold-water bath, and the contents were analyzed by X-ray diffraction to identify the reaction products.

Thick-walled silica tubes (1 mm ID × 4 mm OD) were used to contain the buffered experimental charges. Tubes were first loaded with 200 mg of the powdered PtS mixed with 10 mg of excess Pt powder, then a 10 mm length of 1 mm diameter silica rod and 50 mg of tightly packed silica powder were added to separate the buffer from the sample. Above the packed silica, ~20 mg of the Cu + IPGE metal mixture was packed, with the total mass of metal calculated to be less than that which would consume 50% of the PtS, thus ensuring that both Pt and PtS would always be present to buffer $f(S_2)$. A silica rod was then inserted on top of the metal mixtures, and the tube was evacuated and sealed. A completed sample assembly is shown in Figure 1.

Charges were placed upright, three at a time (Ru–Os Ru–Os–Ir and Ru–Ir), in a bottom-loading furnace (thermal gradient <1°C/5 cm from furnace bottom), and the height of the monitoring thermocouple was adjusted such that it was juxtaposed to the Cu–IPGE mixture. After 70–79 hours, experiments were quenched in a cold-water bath, cut open using a diamond saw, and the run products removed. The remaining Pt–PtS buffer assemblage was mounted in epoxy, and polished for reflected light microscopy and electron-microprobe analysis to test whether PtS and Pt were both present at the end of experiments.

TABLE 1. SUMMARY OF STARTING COMPOSITIONS, CONDITIONS OF EACH EXPERIMENTAL CHARGE, AND PGM PRESENT UPON ANALYSIS

Experiment I.D.	Duration hours	T °C	log $f(O_2)$	log $f(S_2)$	gas-flow rates cm³/min CO-CO_2-SO_2	Buffer	Starting at.% Ru	Os	Ir	Product Lrt	Al
Gas-mixing experiments											
A-1250-1.0	72	1250	-9.0	-1.0	14.2-5.4-8.1	n.a.	75	25	0		×
B-1250-1.0	72	1250	-9.0	-1.0	14.2-5.4-8.1	n.a.	74	12	14		×
C-1250-1.0	72	1250	-9.0	-1.0	14.2-5.4-8.1	n.a.	74	0	26		×
G-1250-1.0	72	1250	-9.0	-1.0	14.2-5.4-8.1	n.a.	90	10	0	×	×
H-1250-1.0	72	1250	-9.0	-1.0	14.2-5.4-8.1	n.a.	90	5	5	×	×
I-1250-1.0	72	1250	-9.0	-1.0	14.2-5.4-8.1	n.a.	91	0	9		×
Erev-1250-1.0*	72	1250	-9.0	-1.0	14.2-5.4-8.1	n.a.	24	49	27		×
A-1200-1.0	70	1200	-9.0	-1.0	4.0-0.0-4.7	n.a.	75	25	0	×	×
B-1200-1.0	70	1200	-9.0	-1.0	4.0-0.0-4.7	n.a.	73	15	11	×	×
C-1200-1.0	70	1200	-9.0	-1.0	4.0-0.0-4.7	n.a.	75	0	25	×	×
Evacuated-silica-tube experiments											
D-1250-0.05	72	1250	n.d.	-0.07	n.a.	Pt/PtS	23	77	0	×	×
E-1250-0.05	72	1250	n.d.	-0.07	n.a.	Pt/PtS	25	37	38	×	×
E-1250-0.05 for reversal*	72	1250	n.d.	-0.07	n.a.	Pt/PtS	24	49	27	×	×
F-1250-0.05	72	1250	n.d.	-0.07	n.a.	Pt/PtS	30	0	70	×	×
D-1200-0.37	72	1200	n.d.	-0.39	n.a.	Pt/PtS	21	79	0	×	×
W-1200-0.37	79	1200	n.d.	-0.39	n.a.	Pt/PtS	50	25	26	×	×
F-1200-0.37	72	1200	n.d.	-0.39	n.a.	Pt/PtS	33	0	67	×	×

Symbols: n.d.: not determined, n.a. not applicable, Lrt: laurite, Al: alloy. * denotes experiment run first at log $f(S_2) = -0.07$ and then re-run at log $f(S_2) = -1.0$.

Analytical Conditions

Run products from both types of experiment consisted of solid ingots containing the quenched CuS melt and the IPGE metal + sulfide assemblage. Ingots were mounted in epoxy, sectioned, then polished using 240 and 600 grit silicon carbide and 1 μm alumina powder. The final polish was applied using an automated polishing wheel with 1.0 μm diamond paste. Phases were analyzed using a Cameca SX50 electron microprobe at the University of Toronto. Analyses were performed with a focused beam, 20 kV accelerating voltage and 20 nA beam current. Counting times on each X-ray peak ranged from 10 to 20 seconds. X-ray lines used to determine element concentrations were Cu$K\alpha$, S$K\alpha$, Ru$L\alpha$, Os$L\alpha$, and Ir$L\alpha$, with chalcopyrite as the standard for Cu and S, and pure metals for the IPGE. In all cases, a ZAF correction routine was used to convert raw count-rates to concentrations. Owing to the extremely small size (<5 μm) of alloy produced in some experiments, we monitored beam impingement on the surrounding melt by including sulfur in the analytical routine. Those compositions of alloy with >0.1 wt%

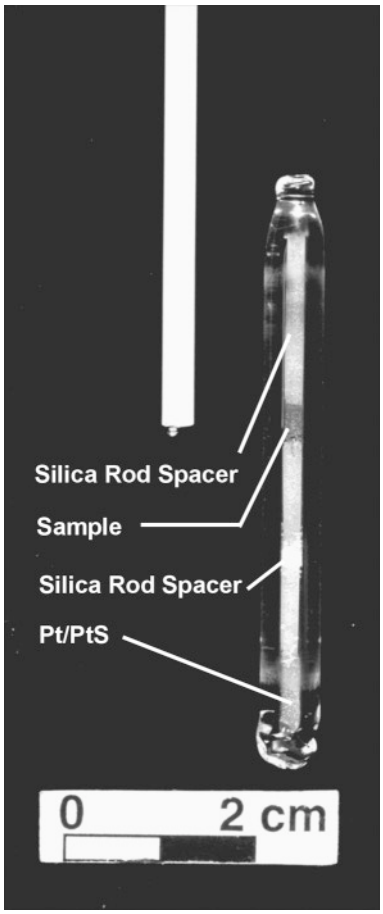

FIG. 1. An evacuated silica-tube assembly is used in experiments done at the Pt–PtS buffer. The Pt–PtS mixture is situated at the bottom of the tube, whereas a silica rod and powder keep the buffer assemblage out of direct contact with IPGE + Cu mixture (dark grey; center of tube). Note the position of monitoring thermocouple bead adjacent to IPGE + Cu sample.

sulfur were considered to have been compromised, and excluded from the final dataset.

RESULTS

Textural and chemical observations of run products

All starting materials were initially sulfur-free, whereas run products clearly show the signs of a reaction with the furnace atmosphere or S vapor produced by the decomposition of PtS, to produce a Ru–Os–Ir alloy ± laurite assemblage surrounded by copper sulfide liquid. For run products in which both laurite and alloy were observed, their Ru, Os, and Ir concentrations plot along tie lines that intersect or come very near the composition of the initial Ru–Os–Ir metal mixture. Slight deviations in tie-line position from initial bulk compositions are attributed to differences in the Cu content of laurite and alloy, and to limited solution of Ru, Os and Ir in the CuS flux. In a given run-product, a visual estimate of the modal proportion of laurite and alloy also suggests behavior in accordance with the lever rule.

The morphology of IPGE alloy phenocrysts was found to vary systematically with their composition (Fig. 2). Grains of alloy in the binary system Ru–Os are relatively small (<10 μm) and subhedral (Fig. 2A), whereas grains of Ir-bearing alloy tend to be larger and more euhedral (Figs. 2B, C). Alloy morphology was also found to be consistent with the known symmetry of the compositions produced. For example, we observed interfacial angles of 90° in the cross-section of alloy grains produced on the Ir-rich side of the field of ternary immiscibility, which is consistent with their face-centered cubic structure. Alloy compositions that lie on the Ir-poor side of the miscibility gap are hexagonal close-packed, and, consistent with this symmetry, we commonly observed six-sided grains in cross-section. Laurite grains produced in experiments are euhedral, and in some cases poikilitic, containing numerous inclusions of alloy. We found that this textural effect could disappear by using Ru-poor bulk compositions; the mass fraction of laurite grown in an experiment was kept to a minimum.

Multiple electron-microprobe analyses across the largest (100–200+ μm) of the laurite and alloy phenocrysts produced in each experiment were done to evaluate their level of homogeneity. Alloy phenocrysts were found to be compositionally homogeneous in most run products, which is also reflected by the low standard deviation in alloy datasets provided in Table 2. Laurite phenocrysts grown from bulk compositions along the Ru–Os binary join showed significant Ru enrichments in the core of larger grains, with a progressive increase in Os concentrations toward the rim. The maximum compositional variation observed for a single grain of laurite is ~20 atomic % Os. Laurite grains grown from ternary or Ru–Ir binary compositions are more homogeneous, with Os or Ir varying by no more than ~2 atomic %. In all experiments, we found that the compositions of small (~10 μm) grains of laurite correspond to that of the rim of larger grains. As such, only small grains of laurite and the rims of large grains are considered to be in equilibrium with the coexisting grains of alloy, and those compositions are provided in Table 2 and plotted in Figure 3.

Inasmuch as all forward experiments involved the production of laurite + alloy from an initial metal mixture, our primary assessment of equilibrium was to "reverse" this phase assemblage, and produce alloy from an initial alloy + laurite assemblage. This was accom-

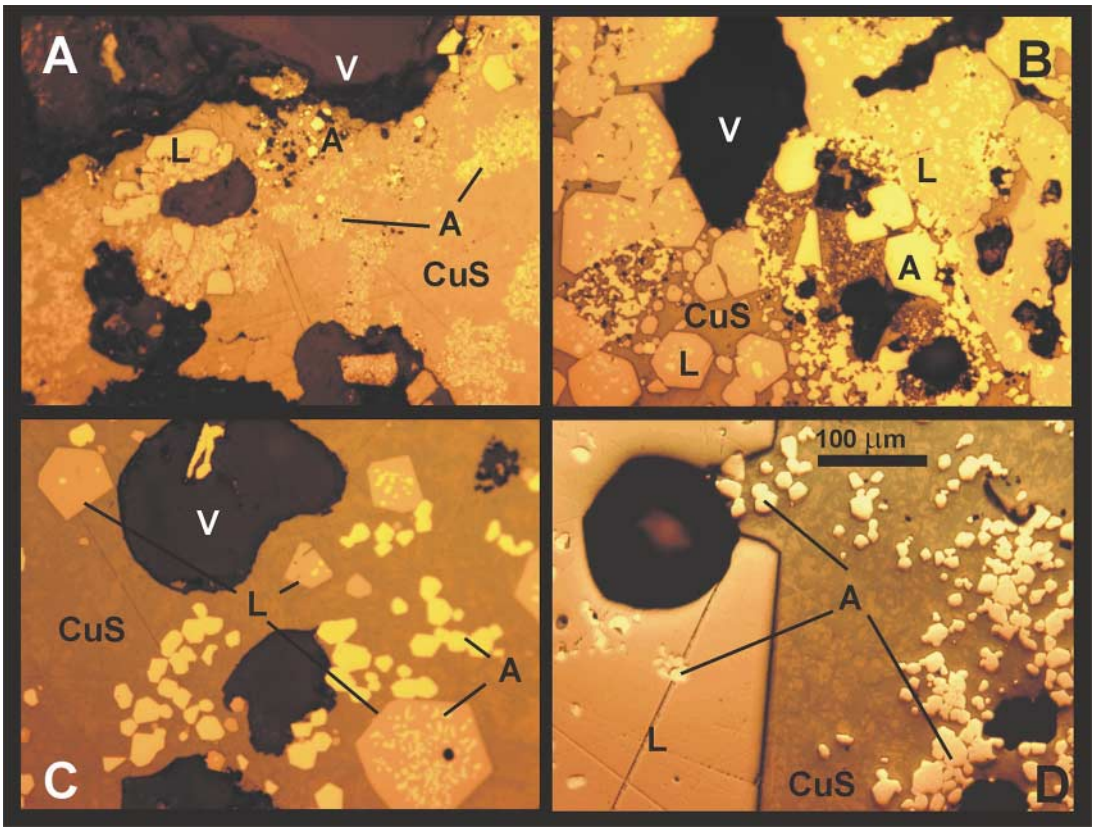

FIG. 2. Reflected-light photomicrographs (plane-polarized light) of sectioned and polished run-products (CuS: quenched copper sulfide liquid, L: Laurite, A: IPGE alloy, V: vesicle). A) Experiment D–1200–0.37. Binary system Ru–Os. Small, anhedral grains of alloy coexist with much larger, euhedral grains of laurite. B) W–1200–0.37. Ternary system Ru–Os–Ir. Abundant inclusions of alloy are present in large, euhedral grains of laurite, along with separate euhedral grains of alloy. C) F–1200–0.37. Binary system Ru–Ir. Note the euhedral development of both laurite and alloy phenocrysts. D) H–1250–1. Ternary system Ru–Os–Ir. Both laurite and alloy exhibit a euhedral morphology.

plished by running two experiments in evacuated silica tubes at 1250°C and log $f(S_2)$ = –0.07, using bulk compositions that had previously been determined to be in the field of laurite + alloy. Upon quenching, one sample was retained for EMP analysis (E–1250–0.05), whereas the other (Erev–1250–1.0), was removed from the silica tube, ground under ethanol, dried, then rerun in an open silica tube in the gas-mixing furnace for 2 days at 1250°C and log $f(S_2)$ of –1.0; such conditions were determined to be in the field of alloy on the basis of "forward" experiments. As expected, laurite is absent in the second experiment, which was confirmed by repeated grinding and polishing. The grains of alloy produced in the second experiment were also slightly richer in Ru than those that were present in the initial experiment with associated laurite, although their composition is still Ru-poor compared to the initial bulk-composition employed.

Effect of temperature on the extent of the laurite + alloy field

To investigate the effect of temperature on the extent of the two-phase field of coexisting laurite and IPGE alloy, experiments were done at 1200° and 1250°C at fixed $f(O_2)$ and $f(S_2)$ of 10^{-9} atm and $10^{-1.0}$ atm, respectively. Compositions of laurite and alloy synthesized in these experiments are portrayed in Figures 3a and b. Letters indicate the initial composition of IPGE in each experiment, and tie lines connect the average composition of coexisting laurite and alloy from each run product. We also did some experiments using Ru-poor compositions to confirm the extent of the stability field of alloy. Consistent with results involving more Ru-rich compositions, only grains of alloy were observed in those experiments.

TABLE 2. SUMMARY OF COMPOSITIONS OF LAURITE AND ALLOY

Experiment I.D.	Phases present Lrt	Al	Phase	n	(element concentrations in wt%) S	Ru	Os	Ir	Cu	Total
Gas-mixing experiments										
A-1250-1.0		×	alloy	4	0.08(0.09)	65.26(5.86)	35.15(5.17)	0.00(0.00)	1.09(1.14)	101.58
B-1250-1.0		×	alloy	6	0.00(0.00)	56.46(10.24)	22.42(20.87)	21.68(10.16)	0.78(0.97)	101.35
C-1250-1.0		×	alloy	13	0.01(0.02)	56.49(3.61)	0.01(0.02)	43.31(3.97)	1.29(0.85)	101.10
G-1250-1.0	×	×	laurite	55	39.24(0.18)	58.91(0.31)	0.20(0.06)	0.03(0.05)	0.06(0.11)	98.45
			alloy	5	0.00(0.00)	76.20(12.32)	24.21(12.37)	0.01(0.02)	1.49(0.30)	101.91
H-1250-1.0	×	×	laurite	66	39.24(0.25)	58.47(0.44)	0.11(0.10)	0.68(0.17)	0.14(0.19)	98.63
			alloy	13	0.00(0.00)	77.94(6.35)	10.99(7.55)	11.41(3.49)	0.68(0.37)	101.02
I-1250-1.0		×	alloy	12	0.00(0.00)	81.79(2.12)	0.08(0.09)	18.48(2.17)	0.93(0.33)	101.02
Erev-1250 -1.0*		×	alloy	15	0.02(0.03)	5.01(1.04)	67.92(6.38)	26.67(6.23)	0.32(0.16)	99.95
A-1200-1.0	×	×	laurite	22	39.00(0.36)	59.14(0.38)	0.68(0.13)	0.02(0.03)	0.40(0.35)	99.25
			alloy	4	0.02(0.02)	48.82(3.65)	51.89(3.63)	0.00(0.00)	0.90(0.11)	101.63
B-1200-1.0	×	×	laurite	18	38.34(0.59)	56.20(1.35)	0.28(0.16)	3.90(1.55)	0.88(0.64)	99.62
			alloy	5	0.03(0.04)	46.47(3.76)	36.93(5.05)	17.56(2.50)	0.59(0.20)	101.61
C-1200-1.0	×	×	laurite	23	38.36(0.55)	55.36(2.12)	0.15(0.14)	4.58(1.64)	1.38(1.57)	99.85
			alloy	13	0.00(0.00)	60.74(1.64)	0.02(0.05)	40.11(1.48)	0.86(0.29)	101.75
Evacuated-silica-tube experiments										
D-1250-0.05	×	×	laurite	16	36.15(0.22)	43.81(0.37)	19.57(0.29)	0.00(0.00)	0.60(0.46)	100.12
			alloy	6	0.03(0.03)	4.40(2.06)	96.18(2.13)	0.00(0.00)	1.19(0.52)	101.79
E-1250-0.05	×	×	laurite	15	37.17(0.33)	47.61(0.65)	3.88(1.41)	10.85(1.40)	0.59(0.36)	100.11
			alloy	29	0.05(0.08)	5.08(0.30)	57.21(2.26)	37.49(2.08)	0.26(0.36)	100.10
E-1250-0.05 for reversal*	×	×	laurite	n.a.	assumed to be near identical to laurite analyses for E-1250-0.05					
			alloy	n.a.	assumed to be near identical to alloy analyses for E-1250-0.05					
F-1250-0.05	×	×	laurite	19	37.34(0.31)	48.66(0.94)	0.05(0.05)	13.48(1.11)	0.12(0.15)	99.65
			alloy	13	0.00(0.01)	7.24(0.62)	0.01(0.02)	92.64(0.61)	0.59(0.53)	100.49
D-1200-0.37	×	×	laurite	9	36.22(0.36)	45.61(0.46)	17.93(0.53)	0.01(0.02)	0.99(0.44)	100.77
			alloy	4	0.09(0.08)	0.93(1.41)	99.25(1.91)	0.00(0.00)	0.57(0.43)	100.84
W-1200-0.37	×	×	laurite	5	36.75(0.29)	47.32(0.83)	6.39(0.74)	7.24(0.15)	0.13(0.05)	98.46
			alloy 1	6	0.05(0.06)	4.85(0.75)	33.00(1.13)	62.34(0.19)	0.18(0.06)	100.43
			alloy 2	42	0.04(0.09)	5.10(3.17)	62.98(5.20)	31.83(3.54)	0.19(0.26)	100.17
F-1200-0.37	×	×	laurite	10	37.26(0.26)	49.72(0.45)	0.09(0.11)	11.83(0.41)	1.48(0.38)	100.38
			alloy	9	0.00(0.00)	9.10(1.73)	0.00(0.00)	91.84(1.84)	0.18(0.10)	101.13

Standard deviations in parentheses are based on results of n analyses; * denotes experiment run first at $\log f(S_2) = -0.05$ and then re-run at $\log f(S_2) = -1.0$. Symbols: Lrt: laurite, Al: alloy.

At the $f(S_2)$ of these experiments, the two-phase field of laurite + alloy is limited to compositions with $X_{Ru} > 0.80$ at 1250°C and $X_{Ru} > 0.60$ at 1200°C. Laurite produced at these conditions shows only a slight increase in Ir + Os abundances (up to ~3 wt%) with decreasing temperature, *i.e.,* it remains close to end-member RuS_2. At each temperature and bulk composition, we found that Ir is incorporated into laurite more readily than Os.

The composition of coexisting laurite and alloy synthesized at $\log f(S_2)$ of –0.9 to –1.3 and 1200–1250°C in the experiments of Brenan & Andrews (2001a, b) is compared to the results of the current work in Figures 3a and b. In the previous study, we used Fe–Ni–S melt as a growth flux, and experiments contained Pt and Pd, in addition to Ru, Os and Ir. Coexisting laurite + alloy pairs from experiments fRu3, fRu5 and fRu11 (1250°C; $\log f(S_2) = -0.9$ to –1.0) are plotted in Figure 3A. Laurite grains from those experiments are similar in composition to those produced at the same conditions in this study, whereas alloy synthesized in the previous work contains less Ru. Coexisting laurite + alloy pairs from experiments fRu1, fRu2, fRu9, fRu15 and fRu16 (1200°C, $-0.9 > \log f(S_2) > -1.3$) have been plotted in Figure 3B. With the exception of the alloy from experiment fRu9, laurite and alloy compositions are in good agreement with the two-phase field defined in our experiments at 1200°C and $\log f(S_2) = -1.0$. Dissimilarity in the extent of the two-phase field inferred in some of the experiments by Brenan & Andrews (2001a) is probably the result of small differences in the $f(S_2)$ employed, and the more complex compositions investigated in that study. Both laurite and alloy from the Brenan & Andrews experiments contain Fe, Ni and Pt, and as such, those added components are likely to af-

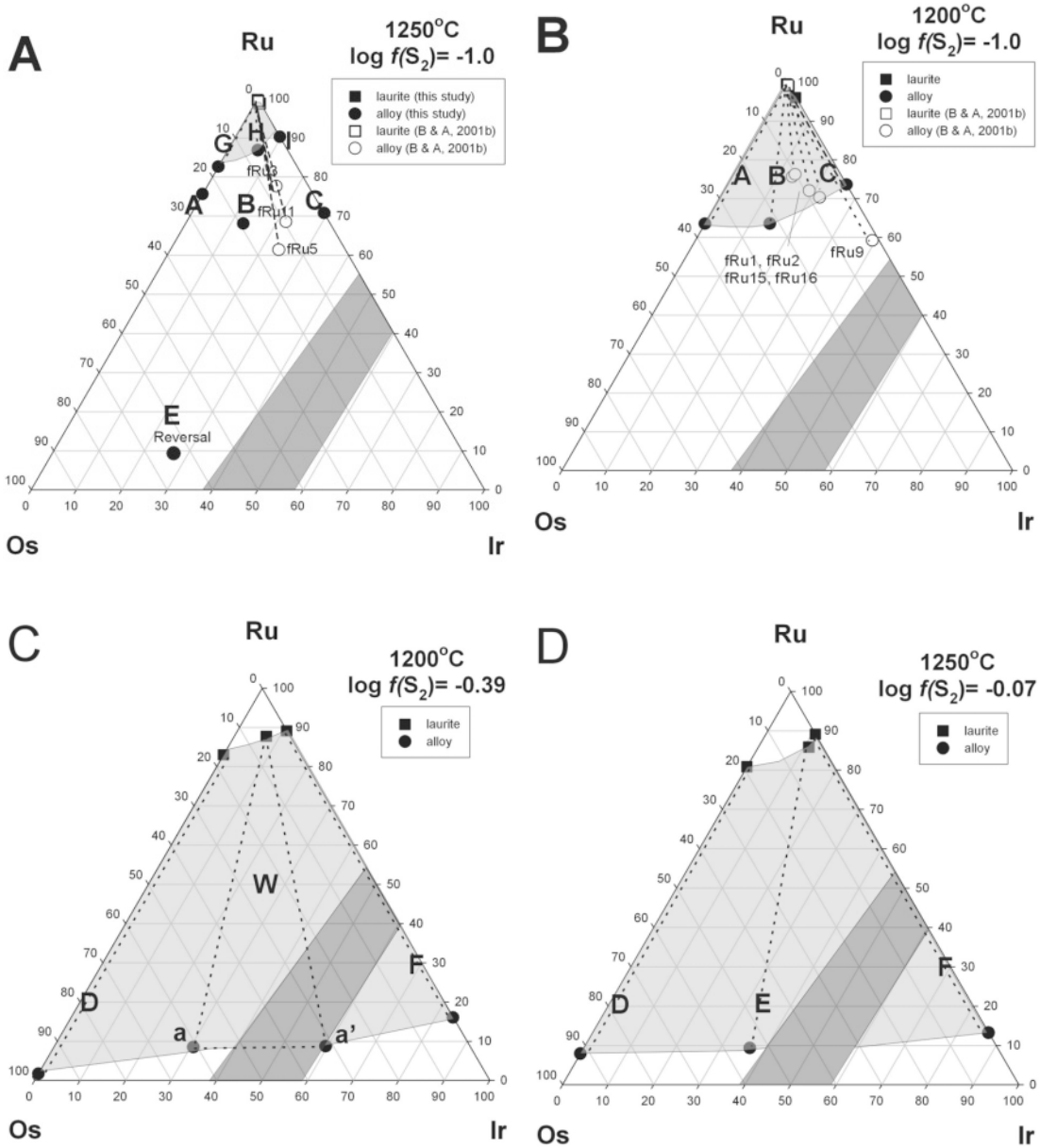

FIG. 3. The composition (atom %) of coexisting laurite and IPGE alloy (light grey field) in experiments done at A) 1250°C, log $f(S_2) = -1.0$; B) 1200°C, log $f(S_2) = -1.0$; C) 1200°C, log $f(S_2) = -0.39$ and D) 1250°C, log $f(S_2) = -0.07$ in terms of the system Ru–Os–Ir. Dark grey region is the estimated ternary miscibility-gap, projected from the solvus limbs in the Ru–Os and Ru–Ir binary systems (Massalski 1990). In all figures, dashed lines connect the average compositions of coexisting laurite and alloy derived from bulk compositions represented by the position of the first letter in their experimental label. Open symbols are data from Brenan & Andrews (2001b), whereas labels indicate corresponding experiments (*i.e.,* fRu9). In 3A), experiment Erev–1250–1.0 (starting composition E) lies in the field of alloy only, after having been reversed from a laurite + alloy assemblage formed at 1250°C and log $f(S_2) = -0.07$. In 3C), the dashed triangle connects two immiscible compositions of alloy associated with a single composition of laurite formed from starting composition W in experiment W–1200–0.37.

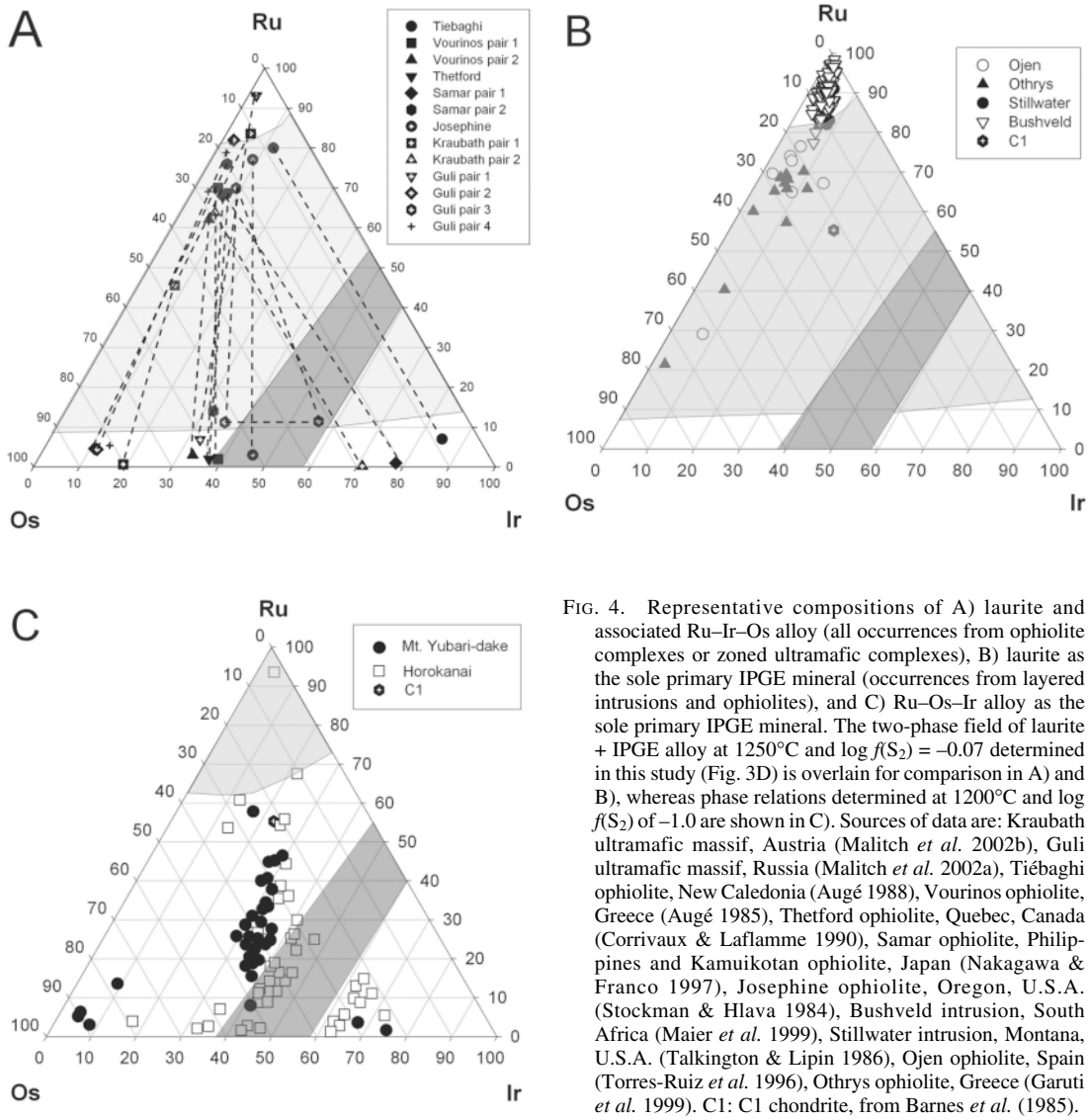

FIG. 4. Representative compositions of A) laurite and associated Ru–Ir–Os alloy (all occurrences from ophiolite complexes or zoned ultramafic complexes), B) laurite as the sole primary IPGE mineral (occurrences from layered intrusions and ophiolites), and C) Ru–Os–Ir alloy as the sole primary IPGE mineral. The two-phase field of laurite + IPGE alloy at 1250°C and log $f(S_2)$ = –0.07 determined in this study (Fig. 3D) is overlain for comparison in A) and B), whereas phase relations determined at 1200°C and log $f(S_2)$ of –1.0 are shown in C). Sources of data are: Kraubath ultramafic massif, Austria (Malitch *et al.* 2002b), Guli ultramafic massif, Russia (Malitch *et al.* 2002a), Tiébaghi ophiolite, New Caledonia (Augé 1988), Vourinos ophiolite, Greece (Augé 1985), Thetford ophiolite, Quebec, Canada (Corrivaux & Laflamme 1990), Samar ophiolite, Philippines and Kamuikotan ophiolite, Japan (Nakagawa & Franco 1997), Josephine ophiolite, Oregon, U.S.A. (Stockman & Hlava 1984), Bushveld intrusion, South Africa (Maier *et al.* 1999), Stillwater intrusion, Montana, U.S.A. (Talkington & Lipin 1986), Ojen ophiolite, Spain (Torres-Ruiz *et al.* 1996), Othrys ophiolite, Greece (Garuti *et al.* 1999). C1: C1 chondrite, from Barnes *et al.* (1985).

fect the activity–composition relations for those phases in complex ways. In general, however, both sets of experiments suggest that at the T–$f(S_2)$ conditions investigated, the two-phase field for laurite + alloy is restricted to relatively Ru-rich compositions.

Effect of $f(S_2)$ on the extent of the laurite + alloy field

To investigate the effect of sulfur fugacity on the extent of the two-phase field of coexisting laurite and IPGE alloy, experiments were done at 1200 and 1250°C at $f(S_2)$ of $10^{-0.39}$ atm and $10^{-0.07}$ atm, respectively. Results are portrayed in Figures 3C and 3D. At these conditions, the laurite + alloy field extends to a X_{Ru} of 0.1–0.2, and the compositional limits of laurite solid-solution expand to a X_{Ru} of 0.8–0.9. Both of these changes represent a considerable shift relative to experiments done at log $f(S_2)$ of –1.0, and are in accord with predictions based on simple thermodynamic modeling of the binary system Ru–Os (Brenan & Andrews 2001). Experiment W–1200–0.37 produced laurite and two compositionally distinct alloys, one Os-rich, and the other Ir-rich (a and a', respectively, Fig. 3C), both with approximately equal Ru contents. Those alloy compositions plot near the limbs of the ternary field of immiscibility, which is defined by interpolation of the

Os–Ir and Ru–Ir solvus limbs (Massalski 1990), and confirmed by the compositions of natural IPGE alloys (Cabri *et al*. 1996).

Discussion and Conclusions

Comparison to natural laurite and Ru–Os–Ir alloy compositions

Compositions of associated laurite and Ru–Os–Ir alloy from natural samples are projected on the Ru–Os–Ir (atomic %) ternary system in Figure 4A. In this case, the term "associated" refers to laurite and alloy that occur as touching grains and as spatially proximal inclusions within the same grain of host mineral (invariably chromian spinel) or, in the case of placer deposits, to samples derived from the same rock formation. In all cases, reported occurrences of associated laurite *and* alloy are from chromitites within ophiolite complexes, with the exception of data from Guli. The Guli ultramafic massif has characteristics of both ophiolitic and zoned ultramafic complexes (K.N. Malitch 2002, pers. commun.). A comparison of Figure 4A with Figures 3A and B shows that the compositions of laurite and alloy in nature tend to be poorer in Ru than compositions produced in our low-$f(S_2)$ experiments. Superimposed on Figure 4A is an example of high-$f(S_2)$ phase-equilibrium data, as defined by experiments at 1250°C and log $f(S_2)$ of –0.07. In contrast to the low-$f(S_2)$ results, the extent of the two-phase field at high $f(S_2)$ shows remarkable similarity with the compositions of natural laurite–alloy pairs. In detail, however, there are some differences. For example, in the most notable of them, several natural laurite–alloy pairs have less Ru than those produced in either of our high-$f(S_2)$ experiments. These pairs may have crystallized at temperatures of 1200–1250°C, but at a higher $f(S_2)$ than our experiments, or they may have formed at similar or lower $f(S_2)$, and have equilibrated at lower temperatures. Given that the temperature range we have investigated is reasonable for the initiation of crystallization of chromian spinel, our results indicate that if natural laurite–alloy pairs were trapped as primary magmatic phases, then the ambient $f(S_2)$ must have been in the range of $10^{-0.39}$ to $10^{-0.07}$ atm.

Figure 4B portrays the composition of natural laurite from parageneses that do not contain any associated Ru–Ir–Os alloy. Laurite in this case occurs both in layered intrusions (Stillwater, Bushveld) and in ophiolites, and in nearly all cases, it occurs as inclusions within a chromian spinel host. Although there is some overlap with the laurite compositions portrayed in Figure 4A, those in Figure 4B tend to be both Ir-poor, and trend to more Os-rich compositions, than laurite associated with Ru–Os–Ir alloy. In comparison to laurite produced in our experiments, even the most Ru-rich laurite in Figure 4B contains more Ir and Os than the compositions we have synthesized at low $f(S_2)$. However, the compositions of laurite from some suites, particularly Bushveld and Stillwater, are consistent with the extent of the laurite-only field as defined by experiments done at high $f(S_2)$. As for the case of the natural alloy–laurite pairs, if laurite entrapment occurred near the chromian spinel liquidus, then high-$f(S_2)$ conditions are inferred. Laurite compositions from the Ojen (Spain) and Othrys (Greece) ophiolites project into the two-phase field defined by our high-$f(S_2)$ experiments. Provided that small amounts of Os–Ir alloy have not been overlooked in these samples, this observation suggests that a higher value of $f(S_2)$ than in our experiments prevailed during crystallization of those suites, or that the laurite formed at a lower temperature.

Data presented in Figure 4C, reported from the Kamuikotan ophiolite belt (Hokkaido, Japan), provide an example of a locality in which alloy is the sole documented host for the IPGE. In this case, nearly all alloy compositions plot within the alloy-only field defined by our low-$f(S_2)$ experiments. This observation would suggest that if the alloy crystallized near the chromian spinel liquidus conditions, then it did so at relatively low fugacity of sulfur, as previously concluded by Nakagawa & Franco (1997).

Comparison with conditions required for sulfide saturation in a basaltic melt

Andrews & Brenan (2002) determined that molten sulfide can dissolve >1000 ppm Ru at magmatic conditions. Further, they concluded that IPGE alloy or laurite would not form in sulfide-saturated silicate magmas, given the low Ru content of igneous rocks. As discussed above, the $f(S_2)$ required to reproduce experimentally the compositions of natural laurite and laurite–alloy pairs at magmatic temperatures is in the range of $10^{-0.39}$ to $10^{-0.07}$ atm, so the question arises as to whether such a high $f(S_2)$ can be reached in natural magmas without its saturation in sulfide melt. The conditions for the formation of a sulfide melt in the presence of a silicate melt can be determined by considering the heterogeneous reaction (Wallace & Carmichael 1992):

$$\tfrac{1}{2}\, O_2 + FeS_{sulf} = \tfrac{1}{2}\, S_2 + FeO_{sil} \qquad (2)$$

where FeS_{sulf} refers to the FeS component in the sulfide liquid in equilibrium with the silicate magma, and FeO_{sil} is the FeO component in the silicate melt. In addition to $f(S_2)$, it can be seen from equation 2 that $f(O_2)$ and the FeO content of the silicate melt also are important variables in determining whether a silicate magma reaches saturation in a sulfide melt. With knowledge of the effects of each of these variables, it should be possible to determine if a "window" exists in $f(O_2)$–$f(S_2)$–X_{FeO} space within which laurite or laurite + alloy may form in the absence of sulfide melt. Unfortunately, owing to limits on the $f(O_2)$ and $f(S_2)$ that can be achieved by gas mixing at high temperature, these effects have not yet been investigated experimentally at high $f(S_2)$. Alterna-

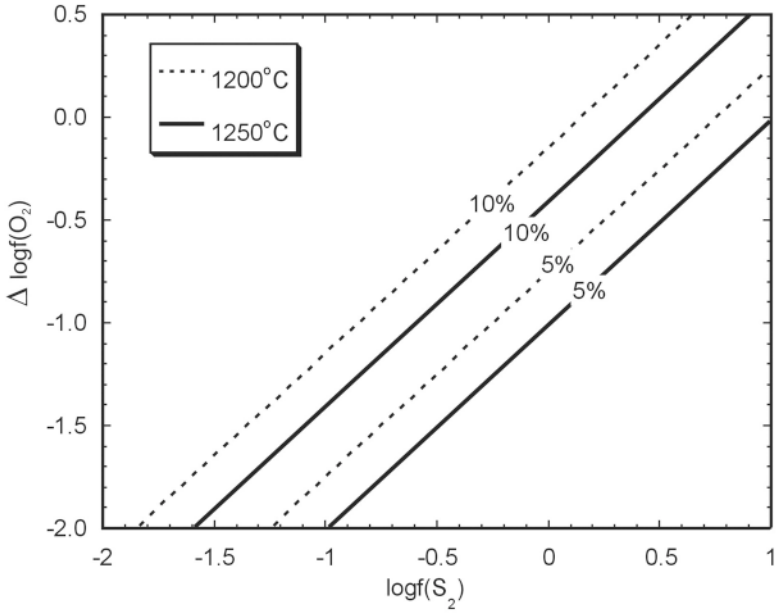

FIG. 5. Calculated $f(O_2)$ and $f(S_2)$ conditions for saturation in a sulfide liquid in a basaltic magma having 5 and 10 mole % total FeO at 1250° (solid curve) and 1200°C (dashed curve). See text for the details of this calculation. Values of $f(O_2)$ on the ordinate are labeled in terms of their log deviation from the fayalite – magnetite – quartz buffer (FMQ).

tively, we can estimate the conditions for sulfide saturation at high $f(S_2)$ by using equation (2) combined with currently available thermodynamic data. We have done this by assuming that the activity of FeS in the sulfide melt is unity, whereas the activity of stoichiometric FeO in the silicate melt is calculated using an activity coefficient of 3.3, as determined by Holzheid *et al.* (1997). In each case, we have adopted a liquid standard state at 1 bar and the T of interest; the equilibrium constant for equation (2) is calculated using the thermodynamic data of Barin (1995). In our calculations, we also assume that all the iron is ferrous, which is reasonable for the $f(O_2)$ range over which calculations were made (Kress & Carmichael 1991).

Figure 5 shows the calculated sulfide-saturation curves for a silicate melt with 5 and 10 mole % FeO at temperatures of 1200 and 1250°C. For our high-$f(S_2)$ experiments, the $f(O_2)$ required for sulfide saturation is FMQ – 0.5 to FMQ – 0.6 in a silicate melt having 10 mole % FeO. Silicate melts having <10 mole % FeO will achieve sulfide saturation at lower $f(O_2)$ for the same values of $f(S_2)$ (*i.e.,* FMQ – 1.0 to FMQ – 1.1 for melts with 5 mole % FeO). Thus, magmas with moderate FeO contents that are more oxidized than ~FMQ – 0.5 will be undersaturated in a sulfide liquid, and capable of producing the observed laurite and laurite + alloy compositions at temperatures near the chromian spinel liquidus. Fe-poor magmas will remain sulfide–liquid-undersaturated to still lower $f(O_2)$. For comparison, the range of $f(O_2)$ values recorded by oceanic basalts is FMQ to FMQ – 2 (median of ~FMQ – 1.3), based on the ferric:ferrous ratio of MORB glasses (compiled in Carmichael 1991). Thus, our calculated $f(O_2)$ values are not unreasonable for natural magmas, suggesting that high $f(S_2)$ could be maintained without saturation in a sulfide melt, although experimental confirmation of such results is clearly needed.

As a final point, it is important to note that some of the suites described in the previous section, particularly Bushveld and Stillwater, have clearly achieved saturation in a sulfide melt during their crystallization history. This observation does not preclude a magmatic origin for laurite from those suites, so long as saturation in a sulfide melt postdated laurite formation and entrapment in chromian spinel. For the case of Bushveld, the absence of laurite as an interstitial phase (Maier *et al.* 1999) seems to support this chronology. Thus, formation of some suites of laurite and laurite + alloy inclusions at the magmatic stage seems plausible, although the $f(S_2)$ required for this to occur is probably near that required for sulfide saturation. The timing of sulfide saturation is clearly a critical factor in determining

whether or not laurite + IPGE alloy are early-crystallizing phases, and if they are to contribute to the removal of PGE in mafic and ultramafic igneous rocks.

Acknowledgements

We are grateful for the thoughtful reviews of W. Maier and A. Borisov, and for the careful editing of R.F. Martin. Funding for this research was provided by the Natural Sciences and Engineering Research Council of Canada. Support for D. Andrews was provided through a Premier's Research Excellence Award.

References

Andrews, D.R.A. & Brenan, J.M. (2002): The solubility of ruthenium in sulfide liquid: implications for platinum-group mineral (PGM) stability and sulfide melt/silicate melt partitioning. *Chem. Geol.* **192**, 163-181.

Augé, T. (1985): Platinum-group-mineral inclusions in ophiolitic chromite from the Vourinos Complex, Greece. *Can. Mineral.* **23**, 163-171.

_____ (1988): Platinum-group minerals in the Tiebaghi and Vourinos ophiolitic complexes: genetic implications. *Can. Mineral.* **26**, 177-192.

Ballhaus, C. & Ulmer, P. (1995): Platinum-group elements in the Merensky Reef. II. Experimental solubilities of platinum and palladium in $Fe_{1-x}S$ from 950 to 450°C under controlled fS_2 and fH_2. *Geochim. Cosmochim. Acta* **59**, 4881-4888.

Barin, I. (1995): *Thermochemical Data of Pure Substances* (3rd ed.). VCH Publishers, New York, N.Y.

Barnes, S.-J., Naldrett, A.J. & Gorton, M.P. (1985): The origin of the fractionation of the platinum group elements in terrestrial magmas. *Chem. Geol.* **53**, 303-323.

Borisov, A. & Nachtweyh, K. (1998): Ru solubility in silicate melts: experimental results in oxidizing region. *Lunar and Planetary Science Conf.* **XXIX**, *Abstr.* 1320.

_____ & Palme, H. (1995): Solubility of iridium in silicate melts: new data from experiments with $Ir_{10}Pt_{90}$ alloys. *Geochim. Cosmochim. Acta* **59**, 481-485.

_____ & _____ (2000): Solubilities of noble metals in Fe-containing silicate melts as derived from experiments in Fe-free systems. *Am. Mineral.* **85**, 1665-1673.

_____ & Walker, R.J. (2000): Os solubility in silicate melts: new efforts and results. *Am. Mineral.* **85**, 912-917.

Brenan, J.M. & Andrews, D. (2001a): High-temperature stability of laurite and Ru–Os–Ir alloy and their role in PGE fractionation in mafic magmas. *Can. Mineral.* **39**, 341-360.

_____ & _____ (2001b): High-temperature stability of laurite and Ru–Os–Ir alloy and their role in PGE fractionation in mafic magmas: erratum. *Can. Mineral.* **39**, 1747-1748.

_____ & Caciagli, N.C. (2000): Fe–Ni exchange between olivine and sulfide liquid: implications for oxygen barometry in sulfide-saturated magmas. *Geochim. Cosmochim Acta* **64**, 307-320.

Cabri, L.J., Harris, D.C. & Weiser, T.W. (1996): Mineralogy and distribution of platinum-group mineral (PGM) placer deposits of the world. *Explor. Mining Geol.* **5**, 73-167.

Carmichael, I.S.E. (1991): The redox state of basic and silicic magmas: a reflection of their source regions? *Contrib. Mineral. Petrol.* **106**, 129-141.

Corrivaux, L. & Laflamme, J.H.G. (1990): Minéralogie des éléments du groupe du platine dans les chromitites de l'ophiolite de Thetford Mines, Québec. *Can. Mineral.* **28**, 579-595.

Garuti, G., Zaccarini, F. & Economou-Eliopoulos, M. (1999): Paragenesis and composition of laurite from chromitites of Othrys (Greece): implications for Os–Ru fractionation in ophiolitic upper mantle of the Balkan Peninsula. *Mineral. Deposita* **34**, 312-319.

Holzheid, A., Palme, H. & Chakraborty, S. (1997): The activities of NiO, CoO and FeO in silicate melts. *Chem. Geol.* **139**, 21-38.

Kress, V. & Carmichael, I.S.E. (1991): The compressibility of silicate liquids containing Fe_2O_3 and the effect of composition, temperature, oxygen fugacity and pressure on their redox states. *Contrib. Mineral. Petrol.* **108**, 82-92.

Legendre, O. & Augé, T. (1986): Mineralogy of platinum-group mineral inclusions in chromitites from different ophiolite complexes. In *Metallogeny of Basic and Ultrabasic Rocks* (M.J. Gallagher, R.A. Ixer, C.R. Neary and H.M. Prichard, eds.). Inst. Mining Metallurgy, London, U.K. (361-375).

Maier, W.D., Prichard, H.M., Barnes, S.-J. & Fisher, P.C. (1999): Compositional variation of laurite at Union Section in the Western Bushveld Complex. *S. Afr. J. Geol.* **102**, 286-292.

Malitch, K.N., Augé, T., Badanina, I.Yu., Goncharov, M.M., Junk, S.A. & Pernicka, E. (2002a): Os-rich nuggets from Au–PGE placers of the Maimecha–Kotui Province, Russia: a multi-disciplinary study. *Mineral. Petrol.* **76**, 121-148.

_____, Thalhammer, O.A.R., Knauf, V.V. & Melcher, F. (2002b): Diversity of platinum-group mineral assemblages in banded and podiform chromitites from Kraubath ultramafic massif, Austria: evidence for an ophiolitic transition zone? *Mineral Deposita* [published online August 17: DOI 10.1007/S00126-002-0308-1].

MASSALSKI, T.B. (1990): *Binary Alloy Phase Diagrams*. 3. *Hf–Re to Zn–Zr* (2nd ed.; H. Okamoto, P.R. Subramanian & L. Kacprzak, editors). ASM International, Materials Park, Ohio.

NAKAGAWA, M. & FRANCO, H.E.A. (1997): Placer Os–Ir–Ru alloys and sulfides: indicators of sulfur fugacity in an ophiolite? *Can. Mineral.* **35**, 1441-1452.

POWNCEBY, M.I. & O'NEILL, H.ST.C. (1994): Thermodynamic data from redox reactions at high temperatures. III. Activity–composition relations in Ni–Pd alloys from EMF measurements at 850–1250 K, and calibration of the NiO + Ni – Pd assemblage as a redox sensor. *Contrib. Mineral. Petrol.* **116**, 327-339.

STOCKMAN, H.W. & HLAVA, P.F. (1984): Platinum-group minerals in alpine chromitites from southwestern Oregon. *Econ. Geol.* **79**, 491-508.

TALKINGTON, R.W. & LIPIN, B.R. (1986): Platinum-group minerals in chromite seams of the Stillwater Complex, Montana. *Econ. Geol.* **81**, 1179-1186.

TORRES-RUIZ, J., GARUTI, G., GAZZOTTI, M., GERVILLA, F. & FENOLL HACH-ALÍ, P. (1996): Platinum-group minerals in chromitites from the Ojen lherzolite massif (Serrania de Ronda, Betic Cordillera, Southern Spain). *Mineral. Petrol.* **56**, 25-50.

TOULMIN, P., III & BARTON, P.B., JR. (1964): A thermodynamic study of pyrite and pyrrhotite. *Geochim. Cosmochim. Acta* **28**, 641-671.

WALLACE, P. & CARMICHAEL, I.S.E. (1992): Sulfur in basaltic magmas. *Geochim. Cosmochim. Acta* **56**, 1863-1874.

Received July 14, 2002, revised manuscript accepted November 2, 2002.